C. R. Geoscience 343 (2011) 284–294

Contents lists available at ScienceDirect

Comptes Rendus Geoscience

www.sciencedirect.com

Internal geophysics

Neoproterozoic paleomagnetic poles in the Taoudeni basin (West Africa)

Pôles paléomagnétiques d'âge Néoprotérozoïque dans le bassin de Taoudéni (Afrique de l'Ouest)

Florent Boudzoumou [a,*,b], Didier Vandamme [b], Pascal Affaton [b], Jérôme Gattacceca [b]

[a] *Département de géologie, faculté des sciences, université Marien Ngouabi, BP 69, Brazzaville, Congo*
[b] *CEREGE, Aix-Marseille Université, CNRS, BP 80, Europôle Méditerranéen de l'Arbois, 13545 Aix-en-Provence cedex 04, France*

ARTICLE INFO

Article history:
Received 20 February 2009
Accepted after revision 21 November 2010
Available online 18 February 2011

Presented by Jean Aubouin

Keywords:
Neoproterozoic
Gourma sub-basin
Taoudeni basin
Glaciogenic deposit
Virtual Geomagnetic Pole
Paleolatitude
Snowball Earth

Mots clés :
Néoprotérozoïque
Sous-bassin du Gourma
Bassin de Taoudéni
Dépôt glaciogénique
Pôle géomagnétique virtuel
Paléolatitude
Snowball Earth

ABSTRACT

A palaeomagnetic study was carried out on Neoproterozoic samples from seven sites of the sub-basins of Gourma and Bobo Dioulasso, which include a Marinoan glaciogenic deposit. Magnetic mineralogy is represented essentially by magnetite and hematite. The mean directions of the sites are calculated on the high temperature component (500–670 °C). Two locations provide data constrained by statistical reversal and fold tests and determining Neoproterozoic virtual geomagnetic poles. The palaeolatitudes display very low values which place the West-African craton in the sub-equatorial position during the Marinoan glaciation. This result enhances the Snowball Earth hypothesis, which places most of the continental landmasses, and notably Africa, at low latitudes during the Neoproterozoic.

RÉSUMÉ

Une étude paléomagnétique a été réalisée sur des échantillons du Néoprotérozoïque provenant de 7 sites des sous-bassins du Gourma et de Bobo Dioulasso, au Sud-Est du bassin de Taoudéni et renfermant un dépôt glaciogénique marinoen. La minéralogie magnétique est représentée essentiellement par la magnétite et l'hématite. Les directions moyennes des sites ont été calculées sur la composante de haute température (500–670 °C). Deux sites présentent des directions contraintes par des tests statistiques d'inversion et de pli et déterminant des pôles géomagnétiques virtuels du Néoprotérozoïque. Les paléolatitudes montrent des valeurs très basses qui placent le craton Ouest-Africain en position subéquatoriale pendant la période de mise en place de la glaciation marinoenne. Ces résultats rehaussent l'hypothèse du « *Snowball Earth* » qui place l'essentiel des masses continentales, et notamment l'Afrique, à de basses latitudes pendant le Néoprotérozoïque.

1. Introduction

The West-African craton (Fig. 1) was stabilized at about 2000 ± 200 Ma, at the end of the Eburnean orogeny (Black and Fabre, 1983). It underlies a vast Neoproterozoic to Quaternary cover represented by the Taoudeni Basin. This cover is relatively homogeneous, with a lateral continuity of facies (Deynoux et al., 1978; Trompette, 1973). The Taoudeni basin consists of two circular sub-basins and four troughs (Villeneuve, 2005). The so-called Gourma basin in the South-East is one of the four troughs. The classic lithostratigraphy of the Taoudeni basin is described in the Adrar of Mauritania

* Corresponding author.
E-mail address: florentboudzoumou@yahoo.fr (F. Boudzoumou).

1631-0713/$ – see front matter
doi:10.1016/j.crte.2010.12.001

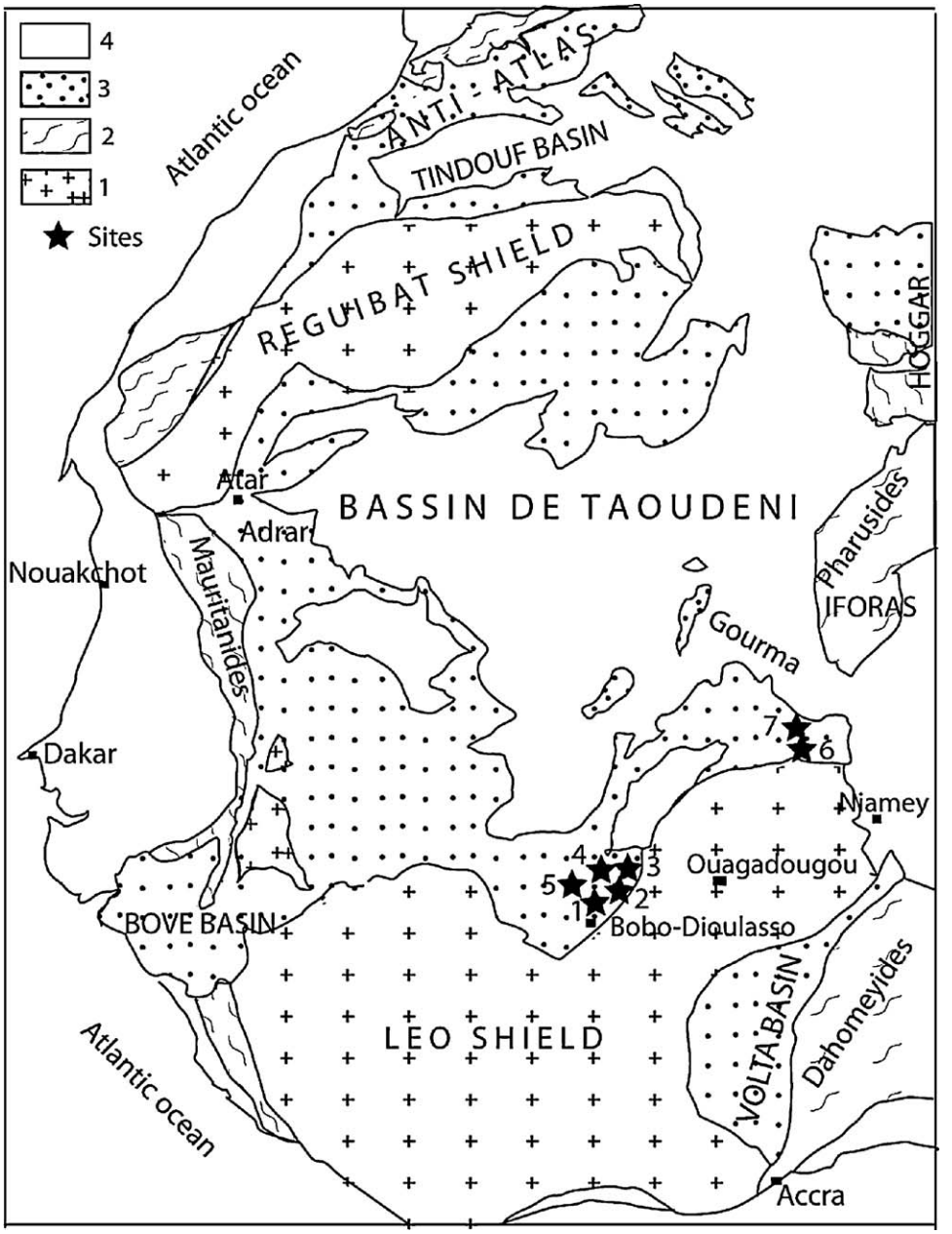

Fig. 1. Schematic geological map of the West-African craton, after Deynoux et al. (2006) simplified. 1- Archean and Paleoproterozoic basement; 2- Pan-African and Caledono-Hercynian fold belts; 3- Neoproterozoic and Paleozoic cover; 4- Post-Paleozoic cover. Sites: 1- Toussiana, 2- Guinguette, 3- Banarodougou, 4-Tiara, 5- Digouera, 6- Tin Dioulaf, 7- Tin Akof.

Fig. 1. Carte géologique schématique du craton Ouest-Africain, d'après Deynoux et al. (2006) simplifiée. 1- Socle archéen et paléoprotérozoïque ; 2- Chaînes plissées panafricaine et calédono-hercynienne ; 3- Couverture néoprotérozoïque et paléozoïque. Sites : 1- Toussiana, 2-Guinguette, 3- Banarodougou, 4-Tiara, 5- Digouéra, 6- Tin Dioulaf, 7- Tin Akof.

(Trompette, 1973). It includes a Neoproterozoic glaciogenic deposit crowned by a "cap carbonate" that is virtually continuous from the central part to the south-eastern one. The cap carbonate does not exist in the south-western part of the Taoudeni basin where there is a high relief (Villeneuve, 2006). The glaciogenic deposit is dated at about 635 Ma (Shields et al., 2007) and testifies to the Marinoan glaciation, one of the two major worldwide glaciations (the Sturtian putting into place between 750–700 Ma and Marinoan glaciations) which have been the basis for the "Snowball Earth" hypothesis (Hoffman and Schrag, 2002; Hoffman et al., 1998; Kirschvink, 1992). These worldwide glaciations may have taken place while all the continental blocks, resulting from the break-up of the Rodinia Supercontinent, were still at low latitudes (Hoffman and Schrag, 2002; Hoffman et al., 1998; Kirschvink, 1992).

In the research for the palaeolatitudes of deposition of glaciogenic rocks, paleomagnetic methods are the most

reliable. They allow the geographic positions of continental blocks during their evolution in the history of the earth to be constrained. The West-African craton is characterized by a meagre palaeomagnetic database, which cannot allow the determination of its Neoproterozoic palaeolatitude with certainty. And some available Neoproterozoic poles were perhaps mostly remagnetized in the Permian (Evans, 2000; Perrin and Prévot, 1988).

The data presented in this paleomagnetic study come from samples of Neoproterozoic formations of the Gourma sub-basin and its Bobo Dioulasso prolongation and are reported in lithostratigraphic section (Fig. 2 b,c) (Miningou, 2006; Ouédraogo, 1983).

Two primary paleomagnetic poles, constrained by folding and reversal tests, are proposed and lead to determine the paleolatitude of the West-African craton during the Neoproterozoic.

2. Geology

The Gourma sub-basin forms the southeastern portion of the large Taoudeni basin and is bounded to the east by the nappes of the Gourma belt. In the adjacent Bobo-Dioulasso region, the lithostratigraphic sequence is composed of three unconformable groups (Fig. 2a; Ouédraogo, 1983). The lower group is about 1200 m thick and consists of fine to medium-grained sandstones or quartzitic sandstones, siltstones and conglomeratic horizons. The middle group is about 1400 m thick and contains fine to coarse-grained quartzitic sandstones, conglomerates with glaciogenic characteristics, shales, glauconitic siltstones, dolomites, stromatolite-bearing dolomitic limestones and silexites. The upper group is thinner, about 50m, and consists of coarse-grained reddish sandstones, conglomerates and fine to medium-grained quartzitic sandstones. In the Beli area, situated in the North-East of Burkina-Faso, the lithostratigraphy consists of eight formations (Fig. 2b; Miningou, 2006). The lower part is made of quartzitic sandstones with conglomeratic lenses. The middle part contains a triad, consisting of glaciogenic deposit-carbonate-silexitic complex, overlain by a sequence of shales and siltstones, including silexite lenses and limestone and sandstone intercalations. Above is a dolomitic sequence. The upper part contains folded calcschists and quartzo-schists which are perhaps thrust over the underlying formation. The whole is capped by molassic sediment.

3. Palaeomagnetism

Seven sites were sampled (Fig. 1). The 118 core samples collected were prepared in the Geophysics and Planetology laboratory at the CEREGE.

3.1. Method

The collected samples are represented by silexites, siltstones, fine-grained sandstones and carbonates. They were drilled and oriented in situ, then cut off in cylindrical specimens and stored in a non-magnetic chamber. They were subjected to thermal demagnetization to isolate their characteristic remanent magnetization (ChRM). Demagnetization in alternating fields was tried on four samples from In Tangoun and gave unsatisfactory results.

Thermal demagnetization was done using a laboratory furnace. The remanent magnetization was measured using a JR5 spinner magnetometer (Agico) and a SQUID (2G enterprises) cryogenic magnetometer. The magnetic susceptibility of each sample at ambient temperature was measured after each heating stage using a Kappabridge KLY5 (Agico) susceptibilimeter to detect possible mineralogical changes.

Two or three samples from each site have been subjected to rock magnetic studies in order to identify the main ferromagnetic carriers. Three methods were used: (1) Thermomagnetic (susceptibility/temperature) curves were done on powders using an MFK1-MFA susceptibilimeter equipped with a CS3 furnace. Samples were heated to 675 °C in air or argon (with similar results), and then cooled; (2) The thermal demagnetisations of three isothermal remanent magnetizations (IRM) (Lowrie, 1990) were measured using JR5 magnetometer. The IRM was acquired using an MMPM9 field pulse magnetizer; (3) The hysteresis loops were generated using a micromag vibrating sample magnetometer capable of reaching 1 T.

For palaeomagnetic studies, the mean direction of the different components of natural remanent magnetization (NRM) in each specimen has been computed using principal component analysis (Kirschvink, 1980). The mean direction within each site was calculated on statistics method (Fisher, 1953). The data were processed using Paleomac 6.1 software (Cogné, 2003). Statistical folding and reversal tests were made and used to characterize the relative age of magnetization.

3.2. Results

The samples possess a natural remanent magnetization (NRM) showing variable intensity (Table 1). The magnetic susceptibility, measured at ambient temperature after each heating stage, is quite stable and does not show any significant mineralogical transformation.

3.2.1. Magnetic mineralogy

Thermomagnetic curves are reversible or irreversible with a dominant effect by magnetite (Fig. 3), and with the presence of hematite. The irreversible curves show an increase in susceptibility between 400 and 500 °C during heating, and about 580 °C during cooling (Fig. 3b, c) due to mineralogical alteration. The thermal demagnetization of IRM shows the unblocking temperatures situated either at about 575 °C (Figs. 4b–d) or above 650 °C (Fig. 4a), corresponding to magnetite and hematite respectively. Goethite is sometimes identified by a drop at 120 °C in the hard fraction (Fig. 4b). On hysteresis loops (Fig. 5), minerals are still not saturated after application of 1000 mT field. There is slightly wasp-waisted form (Fig. 5a) or a larger form (Fig. 5b) due to coercivity of hematite.

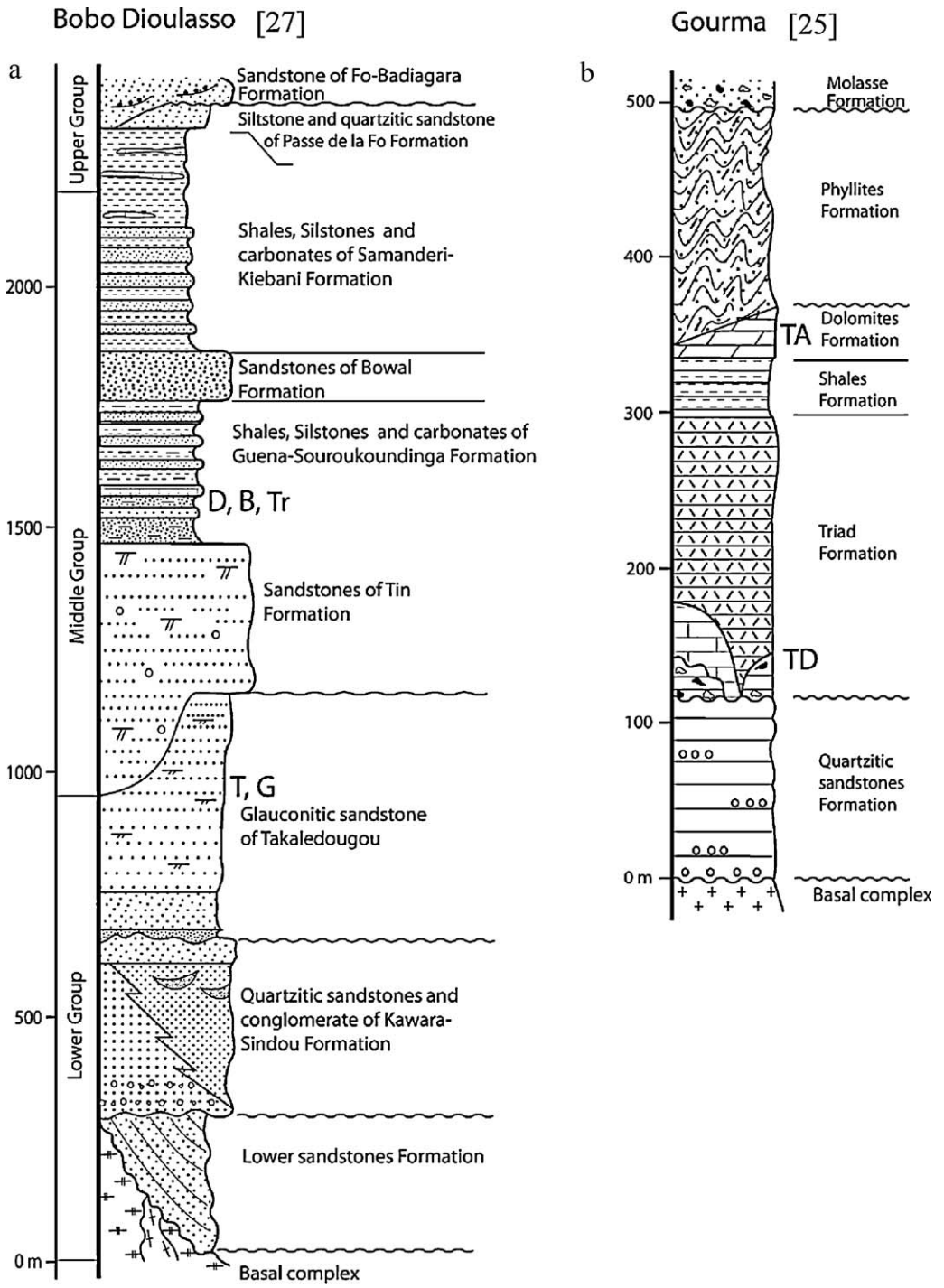

Fig. 2. Lithostratigraphy of the Gourma and Bobo Dioulasso sub-basins: a) from Ouédraogo, 1983; b) from Miningou (2006). Sites: T- Toussiana, G- Guinguette, B- Banarodougou, Tr- Tiara, D- Digouera, TD- Tin Dioulaf, TA- Tin Akof.

Fig. 2. Lithostratigraphie des sous-bassins du Gourma et de Bobo Dioulasso : a) d'après Ouédraogo (1983) ; b) d'après Miningou (2006). Sites : T- Toussiana, G- Guinguette, B- Banarodougou, Tr- Tiara, D- Digouéra, TD- Tin Dioulaf, TA- Tin Akof.

3.2.2. Paleomagnetic analysis

The analysis of principal components reveals one or three components in the rocks (Fig. 6). (1) One component is identified (Fig. 6a$_1$). (2) Two components are identified (Figs. 6a$_2$, 6a$_3$). (3) Three components are identified (Fig. 6a$_4$). In the sample with two or three components, the first or the two first components are destroyed at a low to medium temperature (250–470 °C) when carried by magnetite, and at high temperature (575 °C) when carried by hematite.

Table 1
Mean directions and VGPs of the Gourma and Bobo-Dioulasso sub-basins.

Tableau 1
Directions moyennes et PGVs des sous-bassins du Gourma et Bobo-Dioulasso.

Sites	N/n	Jr	Mx	In situ				After dip correction				South Virtual Geomagnetic Pole						F.T.	R.T.	
												In situ		After dip correction						
		(10-3A/m)		D̂	Î	k1	α95̂	D̂	Î	k2	α95̂	Loñ	Laî	Loñ	Laî	A95̂	Plaî		γĉ	γô
Gourma sub-basin and Bobo Dioulasso																				
Toussiana	9/14	4.9	h	299.6	−23.0	28.2	9.9	300.2	−26.1	27.0	10.1	75.4	−25.9	73.4	−25.9	10.9	−13.8		18.9	18.4
Guinguette	8/11	100	h	323.4	−10.5	10.5	17.9	322.6	−11.5	10.0	18.5	71.9	−50.1	71.7	−49.1	18.8	−5.8			
Banarodougou	15/21	20	m, h	345.2	−7.5	57.8	5.13	345.0	−10.8	75.5	4.4	49.6	−69.0	46.9	−67.6	4.5	−5.4			
Tiara	18/20	5.6	m, h	342.8	−6.9	115.3	3.2	343.1	−2.2	107	3.2	54.6	−67.5	59.1	−69.2	3.2	−1.1			
Digouéra	13/20	4.2	h	345.6	−4.1	12.6	12.1	346.0	−8.6	13.0	11.9	52.8	−70.5	47.3	−69.2	12.0	−4.3			
Tin Dioulaf	10/14	1	m, h	129.3	24.8	12.9	14.0	130.5	16.2	48.5	7.0	63.9	−32.7	68.5	−35.8	7.2	−8.3	+		
Tin Akof	7/18	0.8	m	328.9	9.3	13.2	17.3	332.1	−0.1	14.2	16.6	75.3	−57.8	64.6	−58.8	16.6	−0.1			

N: number of samples used in Fisher's calculation: n: number samples processed; Jr: natural remanent magnetization; Mx: magnetic minerals (m = magnetite, h = hematite); D and I: declination and inclination; K: precision parameter; α_{95}: semi-angle of 95% confidence cone; Lon/Lat: Longitude and latitude of VGP; A_{95}: Fischer confidence angle of the paleomagnetic pole; Plat: paleolatitude; F.T.: fold test; +: Positif fold test; R.T.: reversal test; critical (γ_c) and measured angle (γo) between the direction of the opposite polarity for the reversal test (McFadden and McElhinny, 1990) ($10^\circ < \gamma_c \leq 20^\circ$). The reversal test is positive of class C.

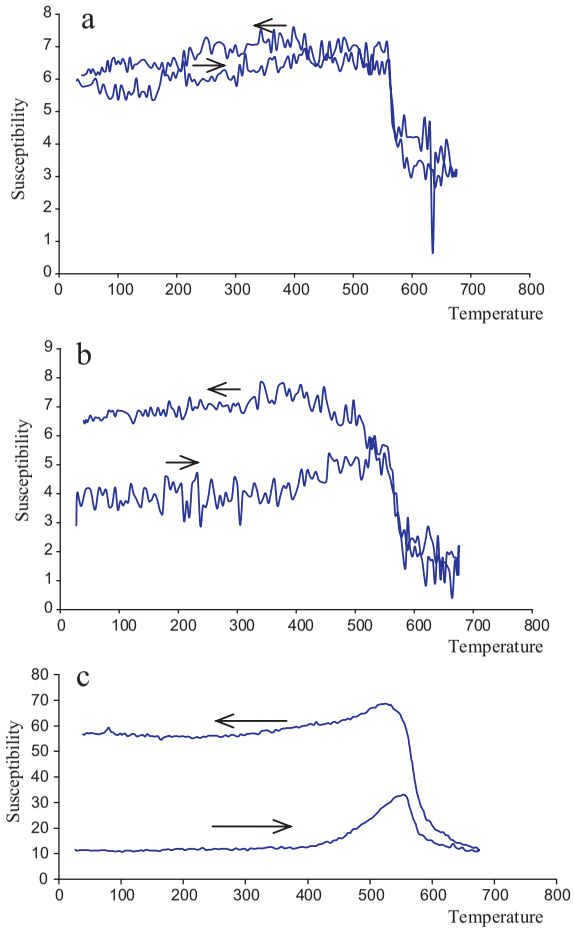

Fig. 3. Susceptibility/temperature curves of the specimens. a) Tiara 7677; b) Tiara 7685; c) Tin Dioulaf 31. Temperature is in degrees Celsius. Susceptibility is in 10^{-6} S.I.

Fig. 3. Courbes de susceptibilité/température des échantillons. a) Tiara 7677 ; b) Tiara 7685 ; c) Tin Dioulaf 31. La température est en degrés Celsius. La susceptibilité est en 10^{-6} S.I.

4. Interpretation and discussion

4.1. Interpretation

The mean paleomagnetic directions are measured on the high temperature component and reported in situ and after dip correction (Table 1 and Fig. 7).

The Toussiana site displays two groups of components, one group with normal polarity and another group with reverse polarity (Fig. 7a). A reversal test (McFadden and McElhinny, 1990) to check the lack of superimposition of several components (Henry et al., 2004) is applied at this site. The angle separating the mean direction of these two components $\gamma_o = 18.4^\circ$, is lower than the critical angle $\gamma_c = 18.9^\circ$. The reversal test is positive of class C ($10^\circ < \gamma_c \leq 20^\circ$).

The Guinguette site gives a mean direction of normal polarity (Fig. 7b) with precision parameter very similar in situ and after dip correction. No statistic test is usable.

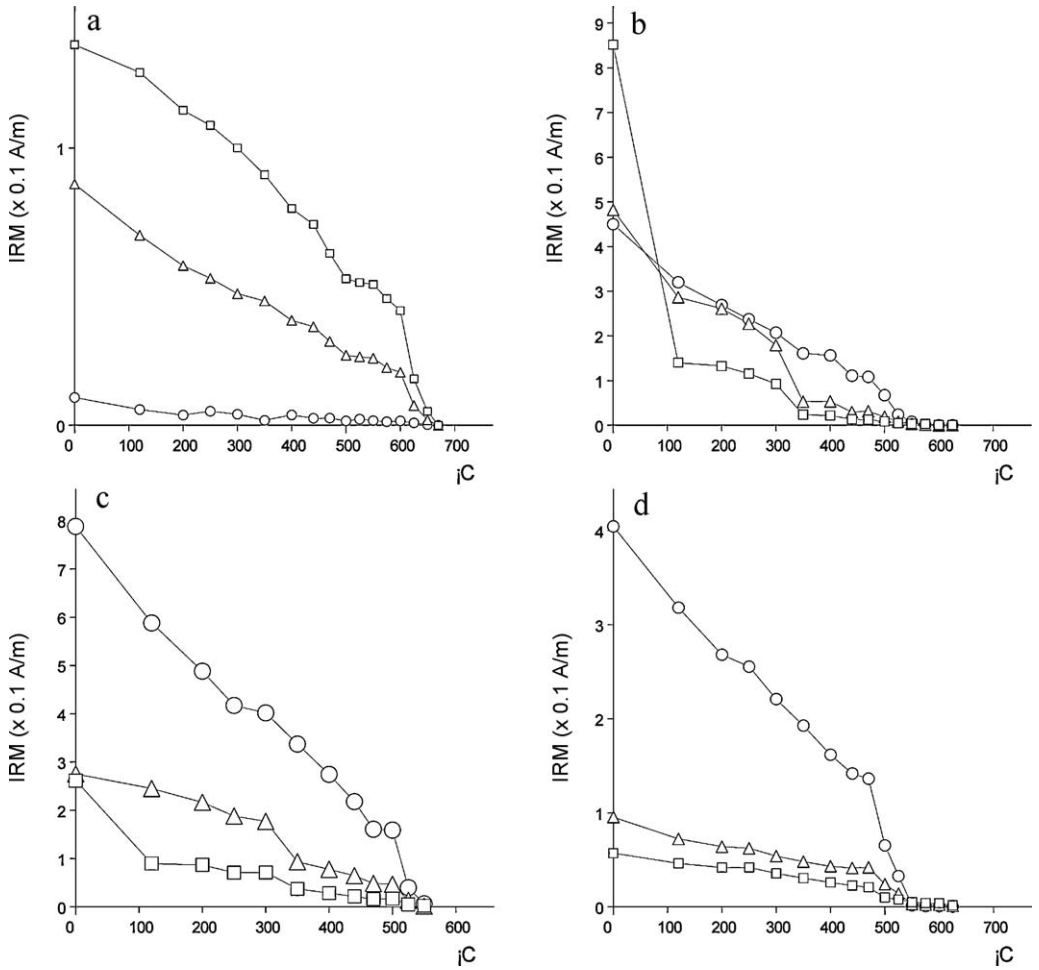

Fig. 4. Example of thermal demagnetization of three axes of isothermal remanent magnetization based on Lowrie (1990) method applied to some samples. : Hard fraction, Δ: Medium fraction; O: Soft fraction. (a) TD: Tin Dioulaf; (b) BAA: Banarodougou A; (c) BAB: Banarodougou B; (d): TR: Tiara.

Fig. 4. Exemple de désaimantation thermique des trois axes de l'aimantation rémanente isotherme, basée sur la méthode de Lowrie (1990) appliquée à quelques échantillons. : fraction dure ; Δ : fraction moyenne ; O : fraction molle. (a) TD : Tin Dioulaf ; (b) BAA : Banarodougou A ; (c) BAB : Banarodougou B ; (d) : TR : Tiara.

The Banarodougou, Tiara and Digouera sites gives very close mean directions (Figs. 7c–e) which is consistent with a similar stratigraphic position. These mean directions diverge from those at Toussiana and Guinguette and are between the Tin Akof direction and the present field. The Banarodougou site is located in a folded area. The mean direction shows $k_2 = 75.5$ (after dip correction) higher than $k_1 = 57.8$ (in situ) but the ration k_2/k_1 gives inconclusive tests (McElhinny, 1964; McFadden, 1990) and non-synfolding magnetization. The Banarodougou and Tiara sites display only a component of normal polarity while the two polarities are recorded in Digouera but the scattered directions of reversed polarity do not permit a conclusive reversal test.

The Tin Dioulaf site (Fig. 7f) is also located in a folded area. It represents a Marinoan cap carbonate. All directions present a reversed polarity and the mean gives precision parameters, $k_1 = 12.9^\circ$ in situ and $k_2 = 48.5^\circ$ after dip correction. The ratio $k_2/k_1 = 3.75$ gives conclusive tests at 95% to 99% (McElhinny, 1964) and 95% (McFadden, 1990). The synfolding test is negative. These positive fold tests shows that the magnetization at the Tin Dioulaf site of the Marinoan cap carbonate considered putting into place at about 635 Ma (Shields et al., 2007) was acquired before the Pan-African folding dated in this area between 616 ± 7 Ma and 585 ± 14 Ma (Affaton et al., 2000; Bertrand et al., 1978). This magnetization should therefore be of Neoproterozoic age.

The Tin Akof site (Fig. 7 g) shows two groups of components, one group with normal polarity and another group with reverse polarity but a reversal test (McFadden and McElhinny, 1990) is indeterminate.

The South Virtual Geomagnetic Poles (VGPs) of our sites are compared with those of other sites from the literature in West Africa and Amazonia (Fig. 8). The paleolatitudes have low values situated between 13.4°S and 0.1°S, which place the craton in subequatorial position.

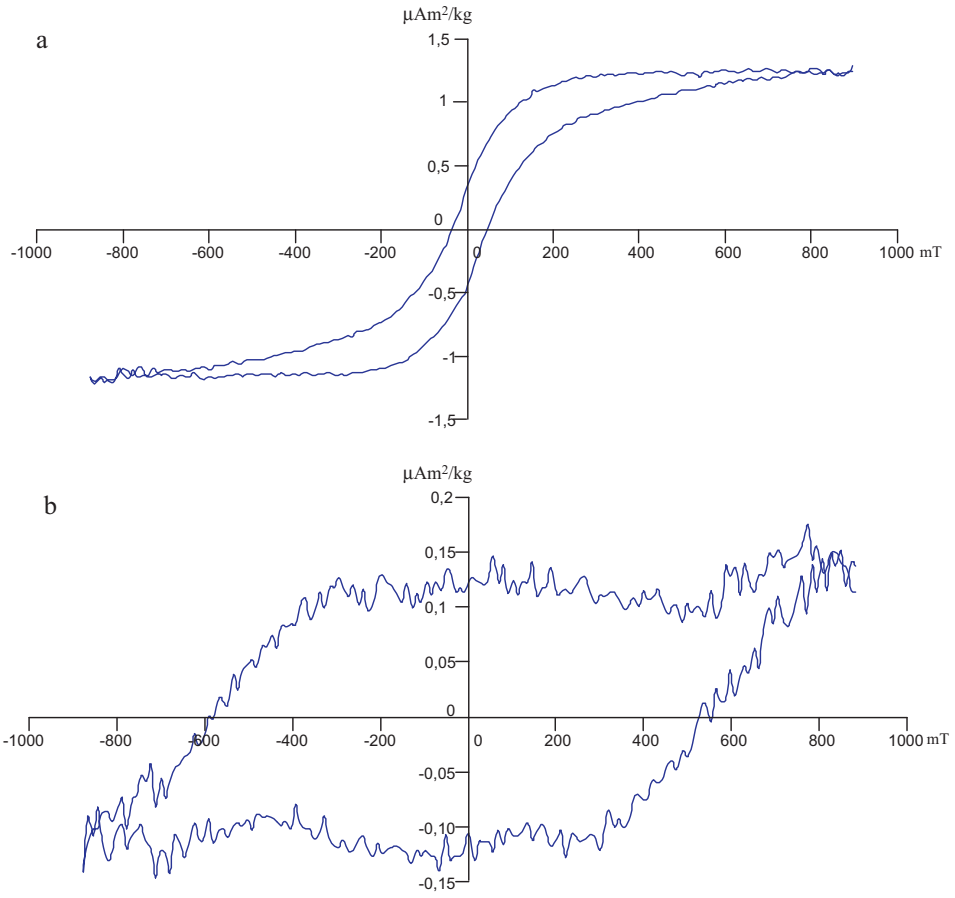

Fig. 5. Hysteresis cycles with slope correction. a: Banarodougou 19; b: Tin Dioulaf 53.

Fig. 5. Cycles d'hystérésis avec correction de pente. a : Banarodougou 19 ; b : Tin Dioulaf 53.

4.2. Discussion

Data processing has shown that the samples carry, often, several magnetization components. The mean minerals, carriers of magnetization, are magnetite and hematite. The mean directions and VGPs are compared with those known in the West-African and Amazonian cratons (Table 2) (Perrin and Prevot, 1988; Perrin et al., 1988; Tohver et al., 2006; Trindade et al., 2003). Some poles in the West-African craton are considered to be Permian remagnetizations (Evans, 2000; Perrin and Prévot, 1988).

In the investigated area, the oldest formations are those at Toussiana and Guinguette sites. These formations are considered as the lateral equivalents of the Assabet el Hassiane Group of the Adrar of Mauritania, whose age is probably posterior to 775 ± 52 Ma (K-Ar age obtained in the underlying Atar Group (Clauer et al., 1982)). The Toussiana results (Table 1) are constrained by the type C reversal positive test. Its VGP coincides with the pole of the Neoproterozoic unit I_9 of the Atar Group (Table 2) considered to have been remagnetized in the Permian (Perrin and Prevot, 1988; Tohver et al., 2006). The Guinguette site gives VGP (Table 1) not constrained by statistical test.

Near the Toussiana and Atar unit I_9 VGPs, is the Tin Dioulaf VGP whose direction was constrained by positive fold test (McElhinny, 1964; McFadden, 1990). The Tin Dioulaf VGP predates the folding of at least one of the Panafrican deformational phases of the Gourma fold belt that affects the "cap carbonate" and the underlying formations. It is a primary pole that postdates 635 Ma, the age of the underlying Marinoan diamictite (Deynoux et al., 2006; Shields et al., 2007). This conclusion is consistent with the position of the Tin Dioulaf VGP close to the VGP of the Puga "cap carbonate" A^d (Trindade et al., 2003) rotated to Africa coordinates using Euler pole rotation (Lawver and Scotese, 1987) see also (Tohver et al., 2006). The Puga cap carbonate A^d dated at 630-580 Ma (Trindade et al., 2003), belongs to the Amazonian craton which coincide to the West-African craton during the Neoproterozoic (Meert and Torsvik, 2003; Rino et al., 2008), after the closure of the Neoproterozoic ocean suggested between those two cratons (Klein et al., 2005; Nomade et al., 2002). The Amouslek tuff VGP, considered as Permian remagnetization, is closed to the Tin Dioulaf. This cluster allows suggesting that Amouslek tuff VGP could be also Neoproterozoic.

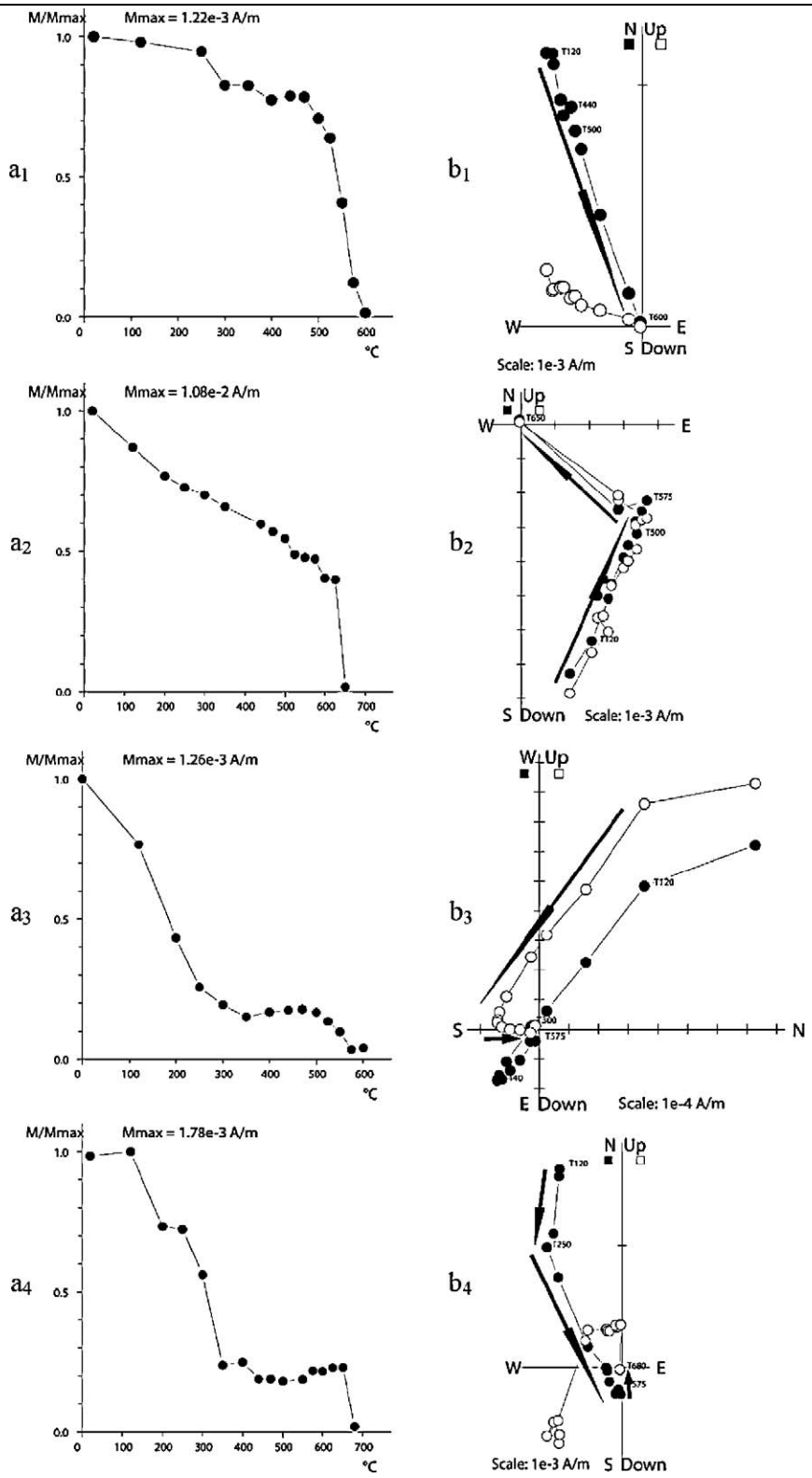

Fig. 6. Thermal demagnetization of characteristic samples: (1) Tiara, (2) Toussiana, (3) Tin Dioulaf, (4) Digouera. a) Intensity curves as a function of temperature ; b) Zijderveld's diagrams (The open/full circles correspond to projections on the vertical/horizontal plane).

Fig. 6. Désaimantation thermique des échantillons caractéristiques : (1) Tiara, (2) Toussiana, (3) Tin Dioulaf, (4) Digouera. a) Courbes d'intensité en fonction de la température ; b) diagrammes de Zijdervelds (les cercles vides/pleins correspondent aux projections sur les plans verticaux/horizontaux).

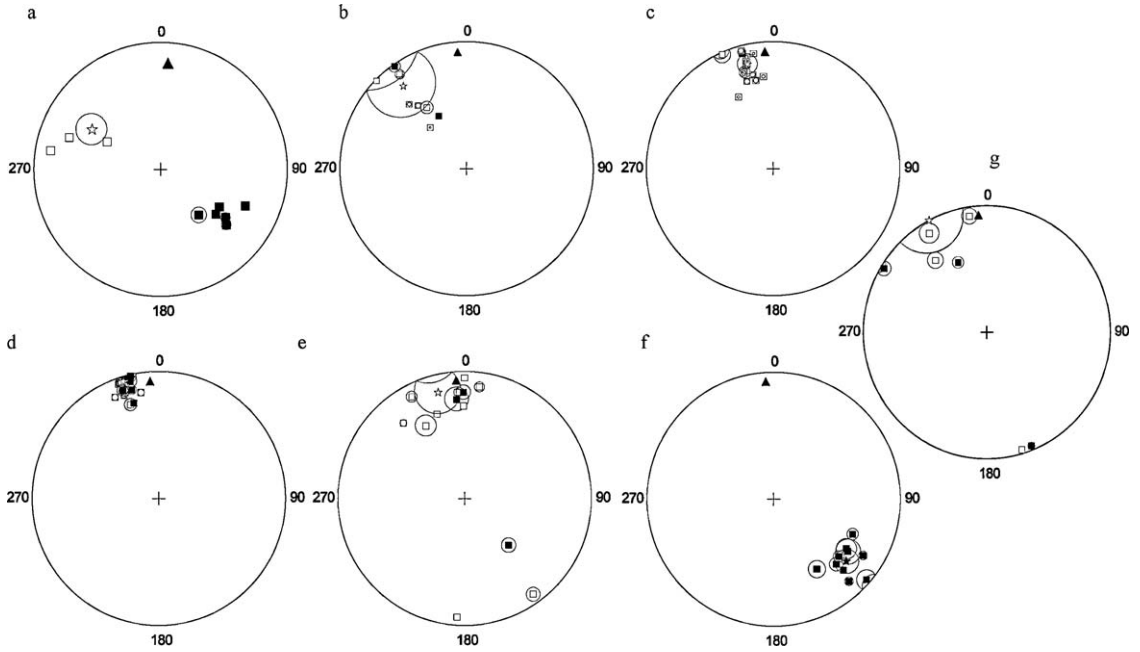

Fig. 7. Stereographic projections of individual directions and the mean of site in the Gourma and Bobo-Dioulasso sub-basins in increasing stratigraphic order: ★(Fisher, 1953) calculated in restoring the data to the same polarity: ■Individual samples; a- Toussiana; b- Guinguette; c- Banarodougou; d- Tiara; e- Digouera; f- Tin Dioulaf; g- Tin Akof.▲: Current geomagnetic field.

Fig. 7. Projections stéréographiques des directions individuelles et moyennes des sites dans les sous-bassins du Gourma et de Bobo-Dioulasso dans l'ordre stratgraphique croissant. ★Fisher (1953) calculé en ramenant les données à la même polarité : ■Échantillons individuels; a- Toussiana ; b- Guinguette ; c - Banarodougou ; d- Tiara ; e- Digouéra ; f- Tin Dioulaf ; g- Tin Akof.▲ : Champ géomagnétique actuel.

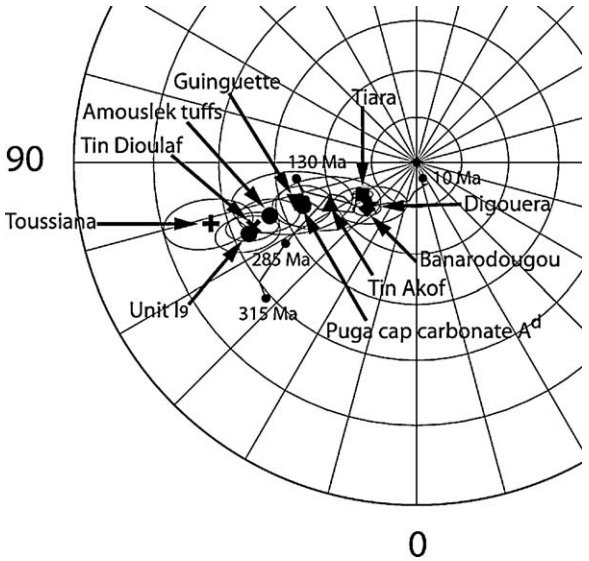

Fig. 8. Paleomagnetic Poles: Comparison of Gourma and Bobo-Dioulasso sub-basins (this study) with some African and Amazonian paleopoles presented in southern hemisphere with African APWP (Cogné, 2003).

Fig. 8. Pôles paléomagnétiques : Comparaison des sous-bassins du Gourma et de Bobo-Dioulasso (cette étude) avec quelques paléopôles africains et amazoniens présentés dans l'hémisphère sud avec l'APWP de l'Afrique (Cogné, 2003).

Banarodougou, Tiara and Digouera sites show closed VGPs (Table 1) which are situated between Tin Akof VGP and the current pole. Without paleomagnetic test these three VGPs could be related to a Late Panafrican deformation remagnetization or possibly to opening Atlantic Ocean but their proximity to the other Neoproterozoic poles permits also to consider a possible primary origin.

The Tin Akof site is stratigraphically above the "Triad". Its VGP (Table 1) diverges from those at Toussiana and Tin Dioulaf and remains near to Puga cap carbonate A^d in Amazonia.

All the sites give relatively low palaeolatitudes (Table 1) situated between 13.4°S and 8.3°N. Such low paleolatitudes were proposed for West-African and Amazonian Neoproterozoic formations (Lefort et al., 2004; Perrin et al., 1988; Trindade et al., 2003). They determine the sub-equatorial position of the West-African craton during the period preceding and following the Marinoan glaciation. The Amazonian craton, which was intimately related to the one in West Africa during its history, in most reconstruction models of the Rodinia and Gondwana supercontinents (Meert and Torsvik, 2003; Rino et al., 2008), is considered to have been at low latitude during the Puga glaciation (Trindade et al., 2003). The low paleolatitudes obtained in the Gourma enhance the "Snowball Earth" hypothesis. Actually, the "Snowball Earth" hypothesis places the continents at low latitudes around the two major (Sturtian and Marinoan) Neoproterozoic glaciations that took place

Table 2
West African and Amazonian Neoproterozoic poles.

Tableau 2
Pôles néoprotérozoïques de l'Afrique de l'Ouest et de l'Amazonie.

Formation	Âge (Ma)		South Virtual Geomagnetic pole		Precision		Reference
	Minimum	Maximum	Long (°)	Lat (°)	dp (°)	dm (°)	
West Africa							
Atar Group I^9	775	866	66.9	−34	4.6	8.6	a, b
Amouslek Tuffs	563	593	70	−41	–	–	c
Amazonia							
Puga carbonate cap A	580	593	69	−51	6	9	d

Data Source: a- Perrin and Prévot (1988); b- Perrin et al. (1988); c- Tohver et al. (2006); d- Trindade et al. (2003).

during the intervals 750–730 Ma and 650–635 Ma (Hoffman and Schrag, 2002; Hoffman et al., 1998; Shields et al., 2007).

5. Conclusion

This palaeomagnetic study, carried out in the South-East of Gourma and Bobo Dioulasso (South-East of the Taoudeni basin), contributes significantly to the knowledge on Neoproterozoic paleomagnetic poles in the West-African craton.

The Toussiana sandstones give a VGP dated at 775 ± 52 Ma. This Toussiana PGV in antipode coincides with the unit I_9 VGP of Atar Group which was considered as remagnetized in the Permian (Perrin and Prévot, 1988; Tohver et al., 2006). The Tin Dioulaf cap carbonate defines a pole with an age close to 635 Ma, which corresponds to the age of the Marinoan tillite on which it reposes (Deynoux et al., 2006; Shields et al., 2007). The Tin Akof carbonates give a younger VGP belonging to the 635–600 Ma interval (i.e. between the age of the underlying formations and the one of the Panafrican orogeny (Affaton et al., 2000; Bertrand et al., 1978; Black et al., 1979; Caby et al., 1982). Banarodougou, Tiara and Digouera VGPs are much more doubtful; they can correspond to a period close to those of Tin Akof but are probably related to later Panafrican deformation remagnetization or a Meso-Cenozoic remagnetization.

Paleolatitudes data place the West-African craton at low latitudes during the Neoproterozoic time.

Acknowledgements

The authors would like to acknowledge the "Bureau des Mines et de la Géologie du Burkina Faso" (BUMIGEB) and the "Institut de Recherche pour le Développement" (IRD), especially A. Blot, for their important help for field work. B. Henry and M. Villeneuve are also acknowledged for their reviews of the first drafts of the manuscript.

References

Affaton, P., Kröner, A., Seddoh, K.F., 2000. Pan-african granulites formation in the Kabye of northern Togo (West Africa): pb-pb zircon ages. Int. J. Earth Sci. 88, 778–790.

Bertrand, J.M., Caby, R., Lancelot, J.R., Mousine-Pouchkine, A., Saadallah, A., 1978. The Late Pan-African intracontinental linear fold belt of the eastern Hoggar (central Sahara, Algeria): geology, structural development, U-Pb geochronology, tectonic implication for the Hoggar shield. Precambrian Res. 7, 349–376.

Black, R., Fabre, J., 1983. In: Fabre, J. (Ed.), A brief outline of the geology of West Africa. Pergamon Press, pp. 19–26.

Black, R., Caby, R., Moussine-Pouchkine, A., Bayer, A., Bertrand, J.M., Boullier, A.M., Fabre, J., Lesquer, A., 1979. Evidence for Late Precambrian plate tectonics in West Africa. Nature 278, 223–227.

Caby, R., Andreopoulos-Renaud, U., Gravelle, M., 1982. Cadre géologique et géochronologique U/Pb sur zircons des batholites précoces dans le gisement pan-africain du Hoggar central (Algérie). Bull. Soc. geol. France 7, 677–684.

Clauer, N., Caby, R., Jeannette, D., Trompette, R., 1982. Geochronology of sedimentary and metasedimentary Precambrian rocks of the West African craton. Precambrian Res. 18, 53–71.

Cogné, J.P., 2003. Paleomac: a Macintosh (application for treating paleomagnetic data and making plate reconstruction. Geochem. Geophys. Geosyst. 4 (1), 1007.

Deynoux, M., Trompette, R., Clauer, N., Sougy, J., 1978. Upper Precambrian and Lowermost Palaeozoic correlations in West Africa and in the western part of Central Africa. Probable diachronism of the Late Precambrian tillite. Geol. Rundsch 67, 615–30.

Deynoux, M., Affaton, P., Trompette, R., Villeneuve, M., 2006. Pan-African tectonic evolution and glacial events registered in Neoproterozoic to Cambrian cratonic and foreland basins of West Africa. J. Afr. Earth Sci. 46, 397–426.

Evans, D.A.D., 2000. Stratigraphic geochronological, and paleomagnetic constraints upon the Neoproterozoic climatic paradox. Am. J. Sci. 300, 347–433.

Fisher, R.A., 1953. Dispersion on a sphere. Proc. R. Soc. Lond. A 217, 295–305.

Henry, B., Merabet, N., Derder, M.E.N., Bayou, B., 2004. Chemical remagnetization in the Illizi basin (Saharan craton Algeria) and their acquisition process. Geophys. J. Int. 156, 200–212.

Hoffman, P.F., Schrag, D.P., 2002. The Snowball hypothesis: testing the limits of global change. Terra Nova 14, 129–155.

Hoffman, P.F., Kaufman, A.J., Halverson, G.P., Schrag, D.P., 1998. A Neoproterozoic Snowball Earth. Science 281, 1342–1346.

Kirschvink, J.L., 1980. The least-squares lines and plane and the analysis of paleomagnetic data. Geophys. J. R. Astron. Soc. 62, 699–718.

Kirschvink, J.L., 1992. Late Proterozoic low-latitude glaciations: the Snowball Earth. In: Schopf, W., Klein, C. (Eds.), The Proterozoic Biosphere. Cambridge University Press, 52 p.

Klein, E.L., Moura, C.A.V., Krymsky, R., Griffin, W.L., 2005. The Gurupi belt in northern Brazil: lithostratigraphy, geochronology and geodynamic evolution. Precambrian Res. 141, 83–105.

Lawver, L., Scotese, C.R., 1987. A revised reconstruction of Gondwanaland. In: McKenzie, G.D. (Ed.), Gondwana Six: Structure. Tectonics and Geophysics. Am. Geophys. Union, Monograph, 40. pp. 17–23.

Lefort, J.P., Aïfa, T., Bourouilh, R., 2004. Évidences paléomagnétiques et paléontologiques en faveur d'une position antipodale du craton Ouest-Africain et de la Chine du Nord : conséquences paléogéographiques. C. R. Geoscience 336, 159–165.

Lowrie, W., 1990. Identification of ferromagnetic minerals in a rock by coercivity and unblocking temperature properties. Geophys. Res. Lett. 17 (2), 159–162.

McElhinny, M.W., 1964. Statistical significance of fold test in palaeomagetism. Geophys. J. R. Astron. Soc. 8, 338–340.

McFadden, P.L., 1990. A new fold test for paleomagnetic studies. Geophys. J. Int. 103, 163–169.

McFadden, P.L., McElhinny, M.W., 1990. Classification of the reversal test in paleomagnetism. Geophys. J. Int. 103, 725–729.

Meert, J.G., Torsvik, T.H., 2003. The making and unmaking of a Supercontinent: Rodinia revisited. Tectonophysics 375, 261–288.
Miningou, M., 2006. Genèse des indices polymétallifères des formations néoprotérozoïques (1000–544 Ma) dans la région du Béli (Burkina Faso) : contrôle structural, nature des fluides, rôle de la silice. Thèse, Université Paul Cézanne Aix Marseille III, 303 p.
Nomade, S., Pouclet, A., Chen, Y., 2002. The French Guyana doleritic dykes: geochemical evidence of three populations and new data for the Jurassic Central Atlantic Magmatic Province. J. Geodyn. 34, 595–614.
Ouédraogo, C., 1983. Étude géologique des formations sédimentaires du bassin précambrien supérieur et paléozoïque de Taoudéni en Haute-Volta. Thèse Université Poitiers, 197 p.
Perrin, M., Prévot, M., 1988. Uncertainties about the Proterozoic and Paleozoic polar wander path of the West African craton and Gondwana: evidence for successive remagnetization events. Earth Planet. Sci. Lett. 88, 337–347.
Perrin, M., Elston, D.P., Moussine-Pouchkine, A., 1988. Paleomagnetism of Proterozoic and Cambrian strata. Adrar de Mauritanie, cratonic West Africa. J. Geophys. Res. 93, 2159–2178.
Rino, S., Kon, Y., Sato, W., Maruyama, S., Santosh, M., Zhao, D., 2008. The Grenvillian and Pan-African orogenes: World's largest orogenies through geologic time, and their implications on the origin of superplume. Gondwana Res. 14, 51–72.
Shields, G.A., Deynoux, M., Culver, S.J., Brasier, M.D., Affaton, P., Vandamme, D., 2007. Neoproterozoic glaciomarine and cap dolostone facies of the southwestern Taoudeni Basin (Walidiala Valley, Senegal/Mali NW Africa). C. R. Geoscience 339, 186–199.
Tohver, E., D'Agrella-Filho, M.S., Trindade, R.I.F., 2006. Paleomagnetic record of Africa and South America for the 1200-500 Ma interval, and evaluation of Rodinia and Gondwana assemblies. Precambrian Res. 147, 193–222.
Trindade, R.I.F., Font, E., D'Agrella-Filho, M.S., Nogueira, A.C.R., Riccomini, C., 2003. Low-latitude and multiple geomagnetic reversals in the Neoproterozoic Puga cap carbonate. Amazon craton. Terra Nova 15, 441–446.
Trompette, R., 1973. Le Précambrien supérieur et le Paléozoïque inférieur de l'Adrar de Mauritanie (bordure occidentale du bassin de Taoudéni, Afrique de l'Ouest). Un exemple de sédimentation de craton. Étude stratigraphique et sédimentologique. Trav. Lab. Sci. Terre St Jérôme, Marseille 7(B), 702 p.
Villeneuve, M., 2005. Paleozoic basins in West Africa and the Mauritanide thrust belt. J. Afr. Earth Sci. 43, 166–195.
Villeneuve, M., 2006. Les dépôts glaciaires néoprotérozoïques et Ordoviciens supérieur de la partie sud-ouest du craton Ouest-Africain: leur cadre géodynamique et paléogéographique. Africa Geosci. Rev. 13 2, 187–212.